International Journal of Research and Development in Engineering Sciences
ISSN: 2582 - 4201(Online) , http://www.ijrdes.com/ , Conference Proceedings
International Conference on Emerging Trends in Engineering, Technology and Management 2025
11-12th April 2025 , www.icetm.in , ICETM 2025 , Hybrid Mode
Viswam Engineering College (Autonomous) , Madanapalle , Andhra Pradesh , India
Conference Proceedings , https://doi.org/10.63328/IJRDES-V7C1-ICETM2025
Regular Issue, Vol. 7, ICETM 2025 , Pages: 105 – 115 , ISBN : 978-81-984440-5-9
Received: 11 January 2025 ; *Accepted:* 09 April 2025 ; *Published:* 26 June 2025
https://doi.org/10.63328/IJRDES-V7CIP16
https://www.youtube.com/watch?v=tcjPVQHQEWY
Conference Paper : Original – Classification Research – Qualitative Research Paper

Analysis of Single Phase Induction motor controlling of an Electric Vehicle through a Reduced Switch Multilevel Inverters

M G Mahesh [1], B R Jayasree [2], M Murali [3], Y Indu Priya [4], K Raju Kumar [5], M Karthik [6], Mohd Akbar [7]

[1-6] Department of Computer Science and Engineering (Cyber Security), Institute of Aeronautical Engineering, Dundigal, Hyderabad, India.
[7] Department of Computing and Information Sciences, School of Computing and Information Sciences, University of Technology and Applied Sciences, Muscat, Sultanate of Oman; mohammed.akbar@utas.edu.om

* *Corresponding Author : M G Mahesh ; mgmahesh@gmaik.com*

Abstract: — Multilevel inverters (MLIs) have gained an increasingly high profile in the area of power electronics because they are compact in their design and high efficiency, particularly in electric vehicles (EVs) and photovoltaic (PV) systems. This study introduces an innovative MLI architecture leveraging the switched capacitor (SC) methodology to generate higher voltage levels with fewer components. By cascading SC units, an inverter design remains streamlined, effectively reducing a need for multiple active switches and gate driver circuits. This results in the more cost-effective, compact, and reliable system. To ensure stable DC voltage from a solar input, the fuzzy logic controller (FLC) is implemented in conjunction with the Single Input Multi Output (SIMO) converter, which boosts an input voltage above a DC link level. A proposed inverter topology is evaluated against other reduced-switch MLI configurations acquired from metrics like total harmonic distortion (THD), efficiency, and component count. Simulations, conducted in MATLAB/Simulink, along with experimental testing under variable load conditions, validate a practicality and performance of a design for use in EVs and renewable energy technologies.

Keywords: EVs, SIMO, THD, MATLAB, FLC, Machine Learning. .

1. Introduction

The rising demand for compact, efficient, and economical power electronics has spurred notable advancements in multilevel inverter (MLI) technologies. MLIs are particularly valued for their capability to deliver high-quality AC output with low harmonic content, making them highly suitable for applications in renewable energy systems, electric vehicles (EVs), and industrial motor drives. Their main advantage is that they the resulting stepped waveform significantly reduces Total harmonic distortion (THD) thus improving power quality over conventional two-level inverters. With a growing integration of renewable sources, especially solar photovoltaic systems, there exists the dire need for inverter designs capable of handling fluctuating inputs, while maintaining performance. The demand for use of EVs also underscores a need for inverter topologies that are both efficient and compact, with simpler control requirements and reduced hardware. Conventional MLIs like cascaded H-bridge, diode-clamped, and flying capacitor inverters often involve the high number of switches and passive elements, leading to increased complexity and cost.

To overcome these limitations, recent research has focused on low-switch-count MLI topologies that preserve high performance while minimizing component use the above-mentioned work presents modernistic MLI structure that employs the switched capacitor (SC) methodology. an approach leverages the cascade configuration of SC cells to achieve elevated output voltage levels with fewer switches and driver circuits, resulting in the smaller footprint,

ISSN: 2582 - 4201(Online) , http://www.ijrdes.com/ , IJRDES, Vol. 7, ICETM 2025 , https://doi.org/10.63328/IJRDES-V7CIP16

reduced cost, and better efficiency particularly advantageous for solar and EV applications. A fuzzy logic controller (FLC) is integrated into a system to enhance dynamic response and regulate an output. By adapting a switching strategy in real-time, a FLC improves voltage stability from solar panels. Additionally, the Single Input Multi-Output (SIMO) boost converter is employed to elevate a variable PV voltage to the steady DC link voltage for inverter operation. Recent literature has explored several alternative MLI designs outside a classical three-type classification. Some topologies use multiple DC inputs or coupled inductors, as in [9]–[13], but face scalability challenges. Other designs using SC-based MLI topologies offer output levels of 5, 7, or 13, as found in [12] and [13], with scalability constraints due to increased switching devices. Although a configuration in [14] allows higher levels, it does so at a cost of added complexity and component count.

In reference [16], the novel SC-based MLI combined with the full bridge is proposed. The five-level inverter using just one switch and two diodes is discussed in [17], but this is hard to extend beyond five levels. Similarly, a design in [18] combines an SC front end with the full-bridge back end, but suffers from high control complexity and increased component usage. High switching losses due to high-frequency operation also pose challenges [51]. Although partial charging of SC units offers potential for output level scaling, its implementation is complex [12]. Designing an SC-based inverter that provides high-frequency output with low harmonics and high efficiency remains the key research challenge [19], especially for EVs where size and weight constraints are critical [20].

The solar panels in the PV system provide a variable DC output. That is routed through the DC-DC converter to an inverter and then to a load [21]. This variability is due to changes insunlight and temperature [22]. Thus, it is essential to make sure that the extraction of maximum power by the use of the Maximum Power Point Tracking (MPPT) [23] method is achieved. normally has been carried out by using the DC-DC converter [24].

Control is essential to maintain a stable DC voltage in PV-fed inverters. Strategies are required. Conventional PI controllers are used in standalone PV setups to adjust a converter's duty cycle based on voltage error [25]. However, MPPT-based control alone may not be sufficient, prompting an exploration of AI-based solutions such as fuzzy logic, particle swarm optimization (PSO), and genetic algorithms (GA) [26]. Selecting an appropriate MPPT technique is non-trivial, as each method comes with its strengths and weaknesses. While hill-climbing (HC) and perturb-and-observe (P&O) methods are widely adopted for their simplicity, they often fall short under partial shading, failing to locate a global maximum power point (GMPP) [27].

Several implementations of MLI integrated with MPPT and the DC link have been proposed, where output control is managed by a load [28] or under steady solar irradiation [29]. MPPT dynamically adjusts panel operation to match an optimal power point, which fluctuates throughout a day due to variations in irradiance and temperature. Consequently, real-time monitoring and tracking of these environmental factors are essential.

This study presents the solar PV-based power system employing the 53-level multilevel inverter combined with the SIMO DC-DC boost converter. A system utilizes the P&O MPPT algorithm to maximize energy extraction. A PV panel output is first fed into a boost converter, which raises a voltage to a desired level before feeding it to an inverter. Through cascading SC units, output levels of 17 and 33 have also been evaluated. A proposed configuration is benchmarked against existing MLI designs with respect to device count, power loss, efficiency, and THD. A system is modeled in MATLAB/Simulink and experimentally validated using the hardware prototype.

2. System Overview

The proposed framework integrates the novel SC-based MLI, the fuzzy logic controller for adaptive control, and the SIMO converter to support renewable energy applications and electric vehicle power systems.

2.1 System Components:

Solar PV Array: Supplies an initial DC voltage, which varies with irradiance and temperature.
SIMO Converter: Boosts and stabilizes voltage to maintain the steady DC link.
SC-Based MLI Topology: Converts stabilized DC into the high-quality multilevel AC output.
Fuzzy Logic Controller (FLC): Dynamically adjusts inverter operation based on real-time conditions.
Load: Represents a system's application (e.g., EV motor or grid-connected AC system).

A block diagram of a full system is provided below:

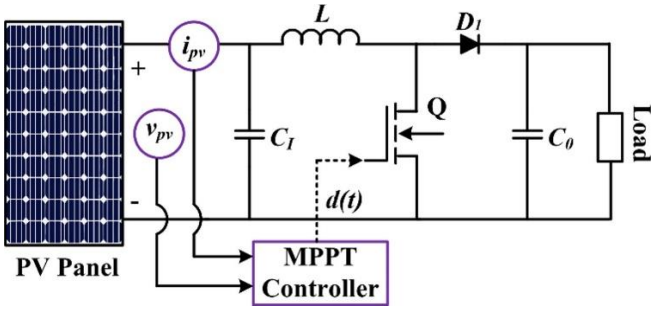

ISSN: 2582 - 4201(Online) , http://www.ijrdes.com/ , IJRDES, Vol. 7, ICETM 2025 , https://doi.org/10.63328/IJRDES-V7CIP16

Note: the simple diagram can be created to show a connections from a solar panel to a SIMO converter, MLI, FLC, and a load.)

2.2 Proposed Multilevel Inverter Topology

a) The proposed inverter topology is based on a SwitchedSC approach uses the cascade, CapacitorConnection of SC cells for obtaining higher output voltagelevels. This design significantly reduces a number of activefewer switches and driver circuits than traditional MLIs.That results in the more compact and cost-effective solution.

b) **Key Features:**

a. **Reduced Component Count: Fewer active it requires switches and passive components. Minimizing cost and complexity.**
b. **High Voltage Output:**a cascade configuration enables a generation of higher voltage levels with Improved output waveform quality.
c. **Improved Efficiency: Reduction of losses by having fewerSwitching devices with simplified control.**

The inverter works by switching capacitors in and out of a circuit to achieve a desired output voltage levels. A switching Pattern is controlled by a FLC to ensure optimal performance under various conditions.

3. Fuzzy Logic Controller(FLC) Analysis

The FLC is used in this work to control an inverter's output voltage and improve its dynamic responseunder various load conditions. A FLC is an intelligent contro lmechanism imitating human reasoning in order to make decisionsbased on imprecise or uncertain inputs.

3.1 Fuzzy Logic Controller Design

c) FLC design involves three key processes namely Fuzzification: Fuzzy sets of crisp input values, like error in output voltage and change in error) are generated, employing membership functions. Rule Base: a set of rules of the form of if-then, where a control strategy is defined by the values of the fuzzy inputs.

d) Defuzzification: This method is applied to restore the crisp Control signal by using the fuzzy output.

e) Inputs to a FLC:

f) Voltage Error (e): a difference between a desired output voltage and an actual output voltage. Change in Error (Δe): a change rate of a voltage error This is an indication of a change in the voltage trend.

g) **Outputs from a FLC:**

2) **Switching Command: Determines which switches in an the inverter should be turned on to achieve a desired output voltage.**

3.2 Membership Functions

The membership functions define how input values are mapped to fuzzy sets. Common linguistic variables used include:

For Error(e): Negative, NB; Zero, ZO; Positive, PB

For Change in Error (Δe): Negative (NB), Zero (ZO),

For Output Switching Command: Strong Negative,Negative (N), Zero (Z), Positive (P), Strong Positive (SP)

Example Membership Functions:

Error (e): Trapezoidal or triangular shapes representing a degree of membership in each fuzzy set.

Δe: Similar shapes, but adjusted to capture rapid changes in error.

3.3 Fuzzy Inference System (FIS)

The FIS is based on the set of fuzzy rules, which determine aninverter's response. An example rule set might look like this:

These rules are applied using a **Mamdani** or **Sugeno** inference

[1] If (e is)	[2] And (Δe is)	[3] Then (Switching Command is)
[4] NB	[5] NB	[6] SP
[7] NB	[8] ZO	[9] P
[10] ZO	[11] PB	[12] N
[13] PB	[14] PB	[15] SN
[16] ZO	[17] ZO	[18] Z

model, with Mamdani being a most common for control applications.

3.4 Defuzzification Process

Once a fuzzy output is derived after using a fuzzy rule, it has to be converted into crisp value. One of the most commonly used defuzzification methods, which is a Centroid Method, computes a center of gravity of an output membership functions to arrive at a final control

$$\text{Defuzzified Output} = \frac{\sum(\mu(x) \cdot x)}{\sum \mu(x)}$$

action.

Where:

μ(x) = Membership degree of output xxx

x = Crisp output value

3) 3.5 FLC Performance in a Proposed System

FLC improves the performance of an inverter by:

Improving Dynamic Response: Rapid adjustment to load changes.

a) Voltage Regulation: Keeps output voltage stable under
b) fluctuating input conditions.
c) Reduced Harmonics: Optimizes switching patterns to
d) minimize THD.
e) Simulation results in MATLAB/Simulink confirm a FLC's
f) effectiveness in stabilizing an output voltage and improving
g) Efficiency at different operating conditions.

ISSN: 2582 - 4201(Online) , http://www.ijrdes.com/ , IJRDES, Vol. 7, ICETM 2025 , https://doi.org/10.63328/IJRDES-V7CIP16

4. Modelling of PV AND DC-DC BOOST CONVERTERA MODELLING OF SOLAR PV

Modeling the solar cell plays an important role in the assessment and optimization of one performance of the photovoltaic system. A configuration proposed here, given in Figure 1, includes solar panels connected to the three-level DC-DC boost converter which in turn feeds the 53-level multilevel inverter(MLI).

The behaviour of the PV system can be analyzed from three
Key insights: Electrical-Equivalent Modeling – Represented through current-voltage (I-V) and power-voltage (P-V)characteristics.

Environmental Influence – Impact of solar irradiance and Ambient Temperature on the PV Output. Partial Shading Conditions – Variability in panel performance under non-uniform lighting.

The term photovoltaic itself puts together two elements: photo(light energy) and voltaic (electrical energy), signifying a photoelectric conversion of light to electricity [30].
A solar array typically consists of multiple modules, with each module containing several solar cells. These cells operate on the principles of p-n junction semiconductor diode [31].

The electric power of the PV module is not fixed- it is highly dependent on environmental conditions like temperature and sun rays [32]. Therefore, the comprehensive solar PV model must account for:
The non-linear I-V and P-V characteristics. Variations due to irradiance and temperature fluctuations. Effects caused by partial shading, which can severely impact performance.

These elements collectively determine a dynamic behavior of a solar PV system and are essential for accurate simulation and control system design.:

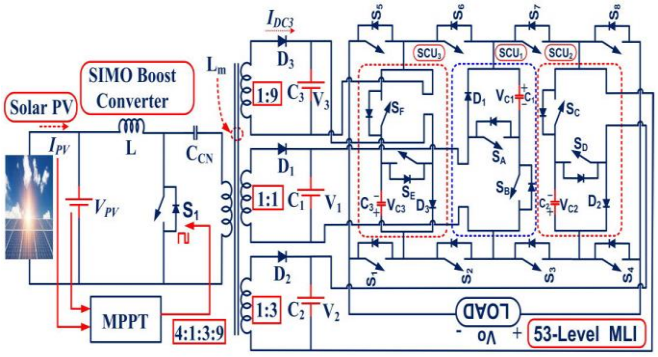

Figure.1 Overall Structure of a proposed system

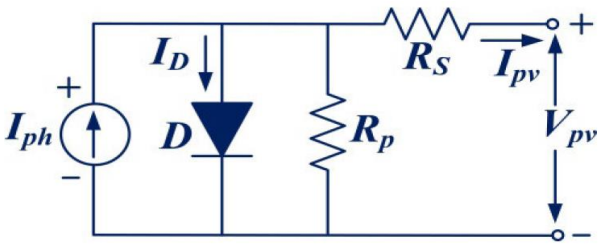

Figure.2 Equivalent circuit of solar cell

SOLAR CELL: EQUIVALENT CIRCUIT AND VI CHARACTERISTICS

solar cell has internal resistance RSE + RSH in series and parallel combination that has also been known as an equivalent circuit as in FIGURE 2. VPV and IPV Key insights: Electricity -Equivalent Modeling -Modeled based on current voltage (Ivoltage) and power voltage (Pvoltance) characteristics,

$$I_{PV} = \left\{ I_{Ph} - I_0 \left[exp\left(\frac{q(V_{PV} + R_{SE} I_{PV})}{N_{SE} AKT} \right) - 1 \right] - \frac{(V_{PV} + R_{SE} I_{PV})}{N_{SE} R_{SH}} \right\} \quad (1)$$

PV cell numbers are linked in series, and also in parallel connections. NSE is a series. Furthermore NSH, RSE are for series, and RH is for parallel resistance, though, sometimes you might find different labels. A factor of 0, 1, and, also, 39 describes a semiconductor device of ideality. K equals the Boltzmann constant. It is about (1.3806503)x10 -23 J/K. And, T, now, is for temperature; this must be known.

Ip is current built. This current, it turns out, is very dependent. The reliance, as is made clear, on irradiation and temperature occurs. And, of course, temperature also. The details appear in equation (2).

$$I_P = [I_{SK-STM} + K_i (T - T_{STM})] - \left(\frac{G}{G_{STM}} \right) \quad (2)$$

ISK stands for short circuit currents at standard testing cases or, more informally, STM. Ki is the short-circuit current coefficient. Now, we need to introduce new terms. G (expressed in W / m 2) defines an irradiance level, actually. It indicates how intensely sunlight touches a cell surface. Furthermore, GSTM(1000 W/ m 2) specifies what amount of radiation can reach STM. Finally the cell temperature, measured specifically, is called TSTM, see [33].

$$I_O = \left\{ \frac{I_{SK-STM} + K_i (T - T_{STM})}{exp\left[(V_{OK-STM} + K_{OV} (T - T_{SKC}) / AV_{Sth} \right]} \right\} \quad (3)$$

VOKSM= open-circuit voltage at test case KOV = open-circuit voltage coefficient, VSth= thermal voltage of solar cell.

$$P_{PV} = V_{PV} \times N_{SH} \left(I_{Ph} - I_O exp\left(\frac{q V_{PV}}{N_{SE} AKT} \right) - \left(\frac{V_{PV}}{N_{SE}} \right) \right) \quad (4)$$

ISSN: 2582 - 4201(Online) , http://www.ijrdes.com/ , IJRDES, Vol. 7, ICETM 2025 , https://doi.org/10.63328/IJRDES-V7CIP16

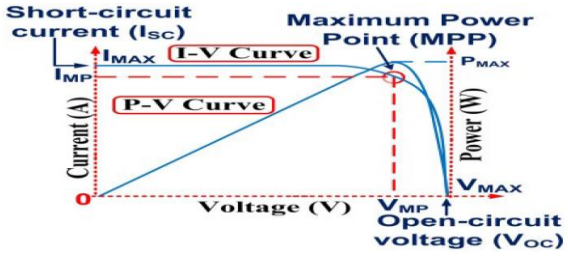

Figure. 3 I-V Characteristics of solar cell

Figure 3 [4] shows the I- V and P- V curves which characterize an electrical mode of action of the solar cell. The curves indicate that a working point of the photovoltaic (PV) module is not constant; it switches constantly between short-circuit current and open-circuit voltage. This range has the individual point where a module produces the highest power at the irradiance level supplied. A voltage and a corresponding current at this maximum power point will be denoted VMPP and IMPP respectively as indicated in Figure 3.

Solar irradiance, cell temperature and a series/ parallel connected cell configuration are some of the factors that determine the PV module outputs voltage and current. Therefore, selecting an appropriate PV panel is essential. In this work, a **1Soltech 1STH-215-P** module is chosen from a MATLAB PV module library, with each string consisting of two modules connected in series and two strings connected in parallel. A specifications of this panel are summarized in **Table 1**, which lists values corresponding to one series module and one parallel string under standard test conditions: 1000 W/m² irradiance and the cell temperature of 25°C.

Influence of Irradiance and Temperature

The output characteristics of the solar PV system vary continuously with changes in environmental conditions [34]. Since irradiance depends on an angle at which sunlight strikes a module, an i–V and P–V curves shift accordingly. As an incident sunlight increases, a PV output current (*IPV*) tends to rise while a voltage (*VPV*) remains relatively stable; under some conditions, VPV may change while IPV stays nearly constant [34].

Temperature also has the significant impact on PV performance. Three main factors contribute to temperature variations in solar cells: (i) heat generated internally during operation, (ii) infrared radiation absorbed by a cell, and (iii) a gradual increase in solar intensity throughout a day [26]. an open-circuit voltage (*VOC*) and short-circuit current (*ISC*) at different irradiance levels can be calculated using equations (5) and (6).

.

$$V_{OC} = V'_{OC} + a_2 (T - T') - (I_{SC} - I'_{SC}) R_{SE} \quad (5)$$

$$I_{SC} = I'_{SC} \left(\frac{G}{G'} \right) + a_1 (T - T') \quad (6)$$

According to an equation provided above, a1 and a2 are temperature coefficients of a PV cell respectively [35]. V0 OC and I0 SCare parameters of reference at G and T0 of the sun. Since changes of climatic conditions are specific, it affects an output voltage and currents. There will be a maximum quantity of power which can be drawn out at any one aspect of a given operation of solar PV. This may be achievable with an efficient MPPT procedure that is based on an temperature and irradiation and provides the constant voltage at an output.

1)
2)

PARTIAL SHADING EFFECT

The partial shading case is also a challenging task of a MPPT technique to achieve maximum power of which is dependent on a conditions of temperature and irradiance. This partial color has mists, one structure after another, trees, etc. [36]. As indicated by equation (2),low insolation decreases a photocurrent Iph. It is a same current in all the cells with series-connected PV modules. However, here a dark cell will be passed to the decomposition and rather than giving out an energy it will serve as the load due to a weakening of photocurrent.

MPPT CONTROLLER

An MPPT controller is used in solar PV operations to maximize power extraction from a PV module. A solar PV's efficiency and lifespan are increased if a controller can effectively track and supply peak power from solar panels during all of the aforementioned disruptions.

Table.1 215W PV system specifications

Maximum power	213.15W
The voltage at maximum power point (V_{MPP})	29V
Open circuit voltage (V_{oc})	36.3V
Current at maximum power point (I_{MPP})	7.35A
Short circuit current (I_{sc})	7.84A
Diode ideality factor	0.98117
Diode saturation current (I_O)	2.9259×10^{-10}A

This will be achieved through sinking a solar source to a load to come up with the most power during varying climatic conditions. conditions. Maximum power will be obtained out of the solar panel methods using two panels. Both of them are electric and mechanical tracking Mechanical tracked solar panels alter their orientation response to the patterns of climatic fluctuation This encompasses different months of weather changes. The work of array is forced to track electrically by an i-V curve in a PV. to find an amplitude of maximum power [37]. A component of a system that produces maximum power to This load (motors or batteries) is known as an MPPT controller. An efficient Maximum Power point Tracking is required to implement (MPPT) algorithm in order to ensure the optimum energy recovery

ISSN: 2582 - 4201(Online) , http://www.ijrdes.com/ , IJRDES, Vol. 7, ICETM 2025 , https://doi.org/10.63328/IJRDES-V7CIP16

of a photovoltaic (PV) Module. This can be expressed as a Power voltage (P-V) characteristics of the solar cell where an optimum is denoted by the clear peak power point (MPP). Some of the MPPT strategies include, Perturb and Observe (P&O), Incremental Conductance. Genetic Algorithms and an Open-Circuit Voltage Fraction method.

In this study, a **Perturb and Observe (P&O)** method is adopted due to its simplicity, ease of implementation, and compatibility with different control platforms such as Arduino and microcontrollers. One of its advantages is an ability to fine-tune a tracking speed by adjusting a perturbation step size. Figure 4 illustrates a flowchart of a P&O algorithm.

P&O Algorithm Workflow:

Measure a PV module's output current (Ipv) and voltage (Vpv).

Calculate an instantaneous power (Ppv = Vpv×Ipv).
Store a current voltage and power readings.
At a next time step (k+1), repeat a measurements.
Determine a changes in power and voltage by subtracting a current values from a previous (kth) values.

On the typical P-V curve, a slope (dP/dV) is negative to a right of a MPP and positive to a left. This means a duty cycle must decrease on a right and increase on a left.
The algorithm adjusts a duty cycle based on a sign of a slope to continuously move toward a maximum power point.

The PV panel used in this system is rated at **215 W**, and its electrical characteristics and specifications are listed in **Table 1**.

DC-DC BOOST CONVERTER

To interface a solar PV module with a proposed inverter, the Single-Input Multi-Output (SIMO) DC-DC boost converter is employed, as depicted in Figure 1 [38]. This converter is designed to produce three isolated DC output voltages in a ratio of 4:1:3:9, ensuring the balanced voltage supply to an inverter.

The SIMO configuration is especially beneficial in addressing an unequal voltage levels that typically arise due to environmental changes such as irradiance and temperature fluctuations. By stabilizing and boosting an input from the
single PV source, a converter allows consistent power delivery to a multilevel inverter while adapting to dynamic climatic conditions.

$$L = \left(\frac{mV_{dc}}{4af_sI_r}\right) \qquad (7)$$

In this expression, Vdc represents an input DC voltage, mmm is a modulation index, fs denotes a switching frequency, Ir is a ripple current, and the is an overload factor, typically taken as 1.25. A required capacitance value can be calculated using a following equation.

$$C = \left(\frac{DI_{dc}}{V_{dc}rf_s \times 0.5}\right) \qquad (8)$$

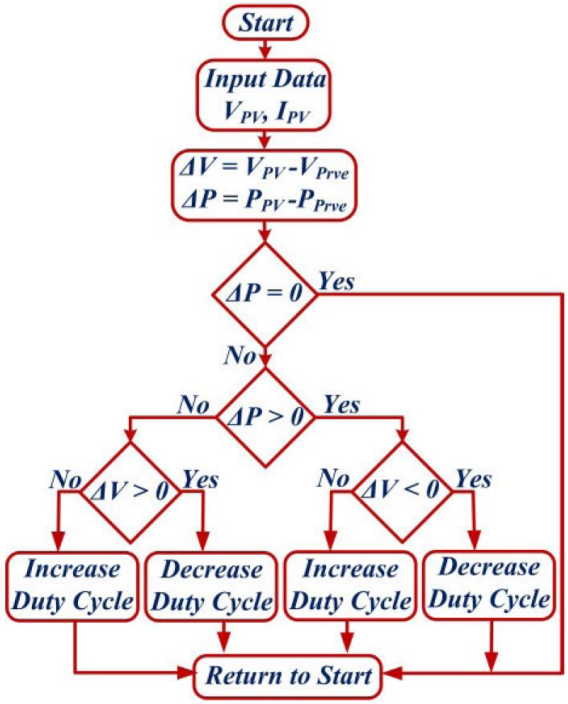

Figure. 4 Flowchart of P&O algorithm

The value of an inductance can be determined using a following relation:

In this equation, Idc is a DC current. And fs is a switching frequency, a point to remember. Where r is the ripple voltage, which may also be delta v; V dc is an input DC voltage. In addition, D is a duty cycle of a converter, which is a critical factor. The duty cycle may be determined by the relationship shown below and is rather simple to execute.

$$D = \left(\frac{V_O}{V_O + V_{dc}}\right) \qquad (9)$$

The proposed system's performance was validated through both simulation, and experimental methods, to some level. The results of the simulations are presented in Figure 5. Now, this is useful and good. Experimental results are shown in Figure 6, the next visual aid, and the following key specs, give details to readers. Certain, important specifications of the boost converter which was utilized in the configuration; is presented too in Table II.

5. Proposed Asymmetrical 17 level MLI

The 17-level inverter proposed here uses an asymmetrical switched capacitor (SC) topology. In this, a SCA network is

ISSN: 2582 - 4201(Online) , http://www.ijrdes.com/ , IJRDES, Vol. 7, ICETM 2025 , https://doi.org/10.63328/IJRDES-V7CIP16

placed at an input stage, followed by an H-bridgeinverter. The SC units operate autonomously as energy storage devices.elements and therefore play the decisive role in determining a voltage.levels of an output waveform.Choosing appropriate capacitance values is important andThat depends on such factors as an operating frequency,
required load current, and acceptable limits of voltage ripple. A unique advantage of the SC-based structure voltage boosting capability enabled by systematic cycling up and down charges without the need for conventional DC-DC converters.

In traditional setups, the DC-DC is usually required to provide the necessary input voltage to an inverter stage. However, in a proposed architecture, the SC network is inherently amplifies a voltage through its sequential action, rendering additional converters superfluous.

By cascading multiple SC units, a topology achieves the stepped output waveform with 17 distinct voltage levels. A design and operation of a MLI are illustrated in a following subsections:

Figure 7(a) presents a fundamental SC unit. Figure 7(b) and Figure 8(a) show a capacitor's charging and discharging cycles. Under optimal operating conditions, a capacitor (C) is charged to the voltage V1 when connected in parallel to a DC source. It discharges its stored energy to a load through the series connection, thereby contributing to a stepped voltage waveform at an output.

6. Result Discussion

Proposed 17-level output voltage waveform with corresponding switching pulses. The waveforms demonstrates a synthesized output voltage waveform. It is of a proposed 17-level MLI during the full cycle of operation.

In Figure 7(a) and Figure 8(a), capacitor C undergoes a charging and discharging process. This happens during each half-cycle. This occurs under optimal operating conditions. Specifically a capacitor C is charged through switch S2 when an output voltage V0=±VC1.

Discharging will start, a touch abruptly, when switch S1 is turned on. This switch occurs at a front end of a proposed MLI topology. During this time, both diode D and switch S2 are turned off. They prevent reverse conduction. In a discharging phase, a voltage sources V1 and VC1deliver energy to a load in combination. A maximum load current delivered during this period can be determined based on a circuit parameters and load conditions, and is given by

$$V_0 = V_1 + V_{C1} \qquad (10)$$

The discharging interval can be utilized to determine an optimal value of a switched capacitor (**SC**) required to achieve a desired ripple voltage across a load. A simulation output waveform illustrating this behavior is presented in **Figure 8(b)**.

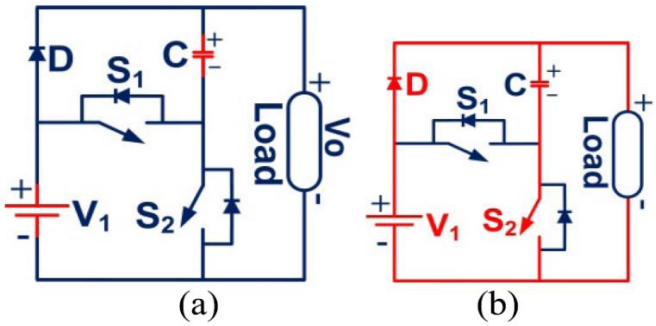

Figure. 7 SCU (a) Basic SC unit: (b) Charging

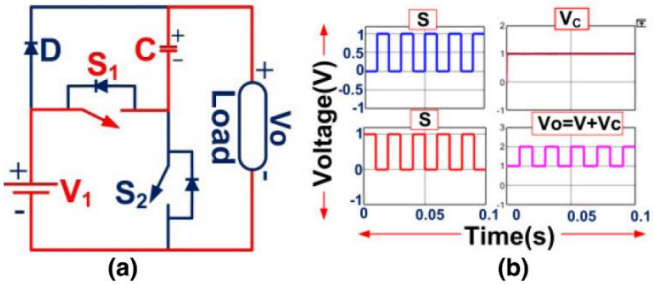

Figure. 8 Capacitor in SC unit: (a) Discharging, (b) Simulation output.

Let QC represent a charge released by capacitor C1 during a discharging period. Then, a charge can be calculated using a fundamental capacitor relation:

$$Q_C = \int_{td1}^{td2} [I_0 sin\,(2\pi fst - \varphi)\,dt] \qquad (11)$$

Where td1 and td2 represent a durations of a capacitor discharging intervals, I0 is a peak output current, fs is a fundamental frequency, and ϕ denotes a phase angle between an output voltage and current. A ripple voltage across a capacitor, denoted as ΔVC, can be determined based on a voltage and current waveforms, particularly by analyzing an angular displacement corresponding to these discharging periods. The angular intervals can be used to estimate a duration over which energy is transferred from a capacitor to a load, and thus help in computing a ripple voltage using:

$$\Delta VC = \frac{1}{2\pi fsC} \int_{\theta}^{\pi-\theta} I0 \sin(2\pi fst - \varphi) d\omega t \qquad (12)$$

Where θ represents a starting angle at which a capacitor begins to discharge, and π−θ indicates an angle at which a discharging process ends.

ISSN: 2582 - 4201(Online) , http://www.ijrdes.com/ , IJRDES, Vol. 7, ICETM 2025 , https://doi.org/10.63328/IJRDES-V7CIP16

17-Level Multilevel Inverter (MLI)

Two cascaded switched capacitor (SC) units are used to implement a 17-level inverter and enable the generation of many levels of output voltage using the fewer components. Figure 9 depicts a scheme of a suggested MLI.

This setup uses 10 controlled semiconductor switches and uses two asymmetric DC voltage sources. Notably, a design eliminates a need for inductors, simplifying a circuit, reducing overall cost and size. A cascaded SC cells function by alternately charging and discharging to raise a voltage levels, allowing an inverter to produce a stepped output. waveform with reduced total harmonic distortion (THD).

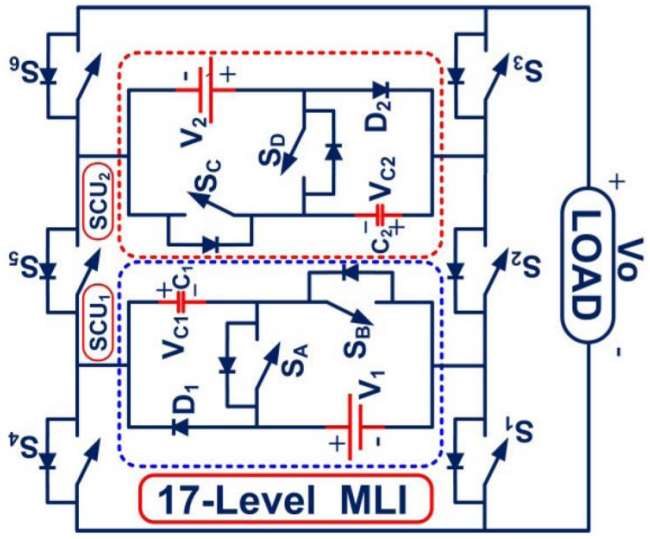

Figure. 9 Developed structure of 17-level MLI.

The proposed 17-level multilevel inverter operates under different switching configurations to achieve stepped output voltage levels. These operational modes are given in detail in Table III, which outlines a corresponding switching state, voltage sources involved, and the resulting output voltages.

Mode 1: Switches **SA, S5, SD, S3, and S1** are turned ON. In this configuration, a voltage sources **V1 (50V), VC1 (150V), V2 (50V), and VC2**

- **(150V)**are connected in series, producing the maximum output voltage of **400V (8Vdc)**.
- **Mode 2**: Switches **D1, S5, SD, S3, and S1** are active. Here, **V1 (50V), V2 (50V), and VC2 (150V)** are utilized, yielding an output voltage of **350V (7Vdc)**.
- **Mode 3**: In this mode, **SD, S3, S6, and S5** are turned ON. A sources **V2 (50V) and VC2 (150V)** are engaged, resulting in an output of **300V (6Vdc)**.
- **Mode 4**: Switches **SA, S5, D2, S3, and S1** conduct, connecting **V1 (50V), VC1 (150V), and V2 (50V)** to form an output of **250V (5Vdc)**.
- **Mode 5**: Switches **D1, S5, D2, S3, and S1** are activated. Voltage sources **V1 (50V) and V2 (150V)** are engaged, generating **200V (4Vdc)**.
- **Mode 6**: an active switches are **D2, S3, S4, and S5**, with only **V2 (150V)** connected, producing **150V (3Vdc)**.
- **Mode 7**: With **SA, S5, S6, and S1** conducting, a sources **V1 (50V) and VC1 (150V)** are used to deliver **100V (2Vdc)**.
- **Mode 8**: a last mode uses **D1, S5, S6, and S1** switches, where only **V1 (50V)** is active, resulting in a minimum step voltage of **50V (1Vdc)**.

Each of these modes corresponds to the distinct voltage level, allowing an inverter to generate the high-quality 17-level stepped waveform. A smart utilization of switched capacitor units enables multiple voltage levels without the proportional increase in a number of switches or passive components.

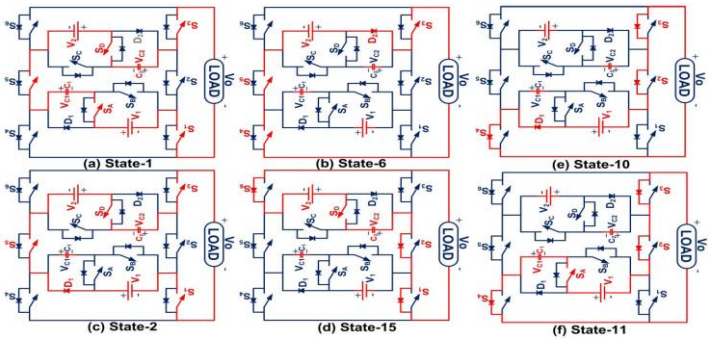

FIGURE 10.Modes of operation of a proposed 17-Level MLI topology.

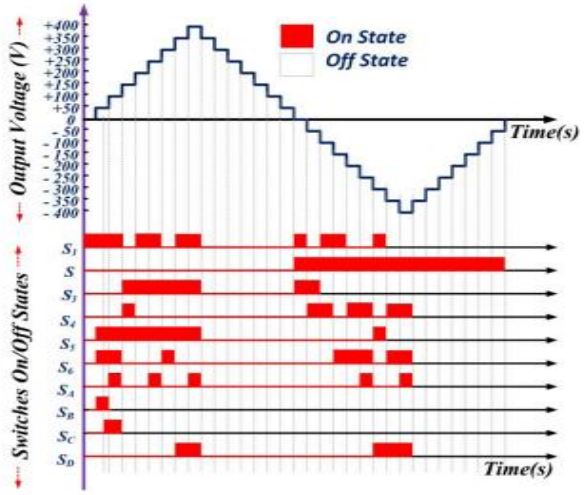

Expected 17-level output voltage waveform with corresponding switching pulses.

The image shows an expected waveform. It is from a 17-level output, also. You will find

ISSN: 2582 - 4201(Online) , http://www.ijrdes.com/ , IJRDES, Vol. 7, ICETM 2025 , https://doi.org/10.63328/IJRDES-V7CIP16

switching pulses depicted there. The figure actually demonstrates something! It presents a synthesized output voltage waveform. The waveform comes from a proposed 17-level MLI during full cycle. It seems like a complete operational demonstration. It's really quite cool you know.an asymmetrical configuration using two unequal DC sources and switched capacitor units allows for generating 17 distinct voltage levels. A waveform shows how various switching combinations sequentially construct a stepped voltage levels, contributing to high power quality and minimized Total Harmonic Distortion (THD). an operation modes correlate with a switching pulses, enabling smooth transition between levels. A design significantly reduces Total Standing Voltage (TSV), component count, and voltage stress across a switches, making a system cost-efficient and compact.

6. Simulation Results

A 17-level Multilevel Inverter (MLI) topology developed with two Switched Capacitor (SC) units laid out in the cascaded structure with the smaller number of units as shown in FIGURE 9. Among the proposed designs is one that has 10 controlled switches and 2 asymmetric DC sources, and an inductor is not used, leading to the small and efficient inverter design.

The asymmetrical configuration of DC sources allows generation of multiple voltage levels by sequential charging and discharging of a SC units. This approach addresses several power quality challenges such as Total Standing Voltage (TSV), Total Harmonic Distortion (THD), voltage stress across switches, and overall cost per level, making a system more efficient in terms of both performance and hardware requirements.

The current path through a switches and a corresponding operational states vary across different modes. an inverter operates in multiple switching modes to synthesize a full 17-level output waveform. Each mode corresponds to the unique combination of source voltages (V_1, V_2) and capacitor voltages (VC_1, VC_2), as determined by an active switches.

Mode-1 Operation: SA, S5, SD, S3, and S1 are enabled and create the path of the load current displaying V1, VC1, V2, and VC2 to an output. All the output voltages add up to a maximum value of 80 V.

Mode-2 Operation: Switches D1, S5, SD, S3 and S1 are on. Here we have V1, V 2 and VC 2 that makes an output, once more, giving a 80 V.

Mode-3: SD, S3, S6 and S5 are switches that are ON. In this case, V 2 and V C 2 would be a source and an output voltage of 80 V is produced. Each of these modes contributes to one of a 17 output levels. A corresponding switching pulses, operational states, and output voltages are detailed further in Table III, while a complete output waveform and its synthesis from these modes are illustrated in FIGURE 11.

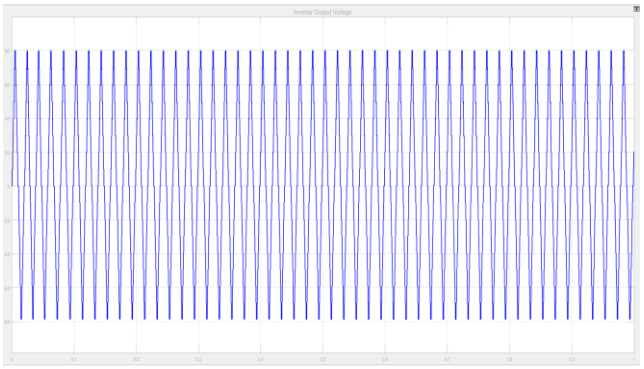

17 Level Voltage output of an inverter Voltage of 80v

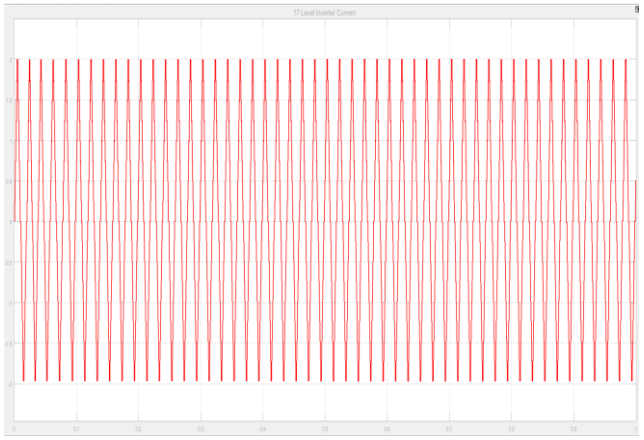

17 Level Current output of an inverter Current of 2A

7. Conclusion

This paper presents the novel multilevel inverter (MLI) topology based on the switched capacitor (SC) configuration, integrated with the fuzzy logic controller (FLC) to improve voltage regulation and dynamic performance in renewable energy and electric vehicle (EV) applications. proposed design reduces a number of active switches and passive components, which yield the more compact, cost-effective, and efficient system compared to conventional MLI topologies. An inclusion of an FLC enables intelligent, real-time switching control, improving system response under under different load conditions. Simulation and experimental results confirm the ability of an inverter to maintain high output voltage quality with reduced total harmonic distortion (THD) and Improved overall efficiency. Comparative analysis with Among the existing reduced-switch MLIs, it demonstrates a superiority of a proposed design in terms of performance metrics such as THD, component count, and voltage stability. These findings validate a proposed MLI as the reliable and scalable solution for

ISSN: 2582 - 4201(Online) , http://www.ijrdes.com/ , IJRDES, Vol. 7, ICETM 2025 , https://doi.org/10.63328/IJRDES-V7CIP16

practical solar PV and EV power conversion applications.

While a proposed system has shown promising results, several areas for further research and development remain:

Advanced Control Strategies: Even more enhanced improvements of dynamic performance and efficiency of an inverter can be made through integration of advocated control algorithms, such as: Model Predictive Control-MPC or Neural Network-based Controllers. Hybrid control approaches which combine FLC with other Intelligent control techniques may offer enhanced Adaptability under complex operating conditions.

Enhanced Topology Optimization: Exploration of new MLI topologies with even fewer components and enhanced voltage balancing techniques Could lead to more cost-effective and compact designs. Implementation of modular multilevel converter (MMC) The structures for high-power applications could be investigated.

Real-Time Hardware Implementation: Development of the real-time hardware prototype using advanced microcontrollers or digital signal processors (DSPs) to validate a performance under more dynamic and complex load conditions. Integration with IoT for Remote monitoring and control of inverter operations.

Energy Storage Integration: Research on integrating a battery management system (BMS) and energy storage devices to improve the system. reliability and support grid stability, especially in off-grid solar applications.

Efficiency Improvement under Extreme Conditions: Investigate a performance of a proposed system under that include extreme environmental conditions: high temperature, irradiance, and load vary widely. demands.

Application in Smart Grids: Exploring the potential of a proposed inverter topology for smart grid applications, both grid-connected and off-grid systems, to support the integration of renewable energy, demand response strategies.

Reference

[1]. X. Wu, C. Xiong, S. Yang, H. Yang, and X. Feng, "A simplified space vector pulsewidth modulation scheme for three-phase cascaded H-Bridge inverters," IEEE Trans. Power Electron., vol. 35, no. 4, pp. 4192–4204, Apr. 2020.

[2]. I. Abari, A. Lahouar, M. Hamouda, J. B. H. Slama, and K. Al-Haddad, "Fault detection methods for three-level NPC inverter based on DC-Bus electromagnetic signatures," IEEE Trans. Ind. Electron., vol. 65, no. 7, pp. 5224–5236, Jul. 2018.

[3]. Mukherjee, S. K. Giri, and S. Banerjee, "An improved adjustable modulation strategy for three-level NPC inverters considering dynamic loading applications," IEEE Trans. Ind. Appl., vol. 55, no. 4, pp. 3915–3925, Jul./Aug. 2019.

[4]. N. D. Dao and D. Lee, "Operation and control scheme to the five-level hybrid inverter for medium-voltage motor drives," IEEE Trans. Power Electron., vol. 33, no. 12, pp. 10178–10187, Dec. 2018.

[5]. Z. Ni, A. H. Abuelnaga, and M. Narimani, "A new fault-tolerant technique based on nonsymmetrical selective harmonic elimination for cascaded H-Bridge motor drives," IEEE Trans. Ind. Electron., vol. 68, no. 6, pp. 4610–4622, Jun. 2021.

[6]. S. A. Singh, G. Carli, N. A. Azeez, and S. S. Williamson, "Modelling, design, control, and implementation to the modified Z-Source integrated PV/Grid/EV DC charger/inverter," IEEE Trans. Ind. Electron., vol. 65, no. 6, pp. 5213–5220, Jun. 2018.

[7]. K. Wang, R. Zhu, C. Wei, F. Liu, X. Wu, and M. Liserre, "Cascaded multilevel converter topology for large-scale photovoltaic system with balanced operation," IEEE Trans. Ind. Electron., vol. 66, no. 10, pp. 7694–7705, Oct. 2019.

[8]. A. Kersten, O. Theliander, E. A. Grunditz, T. Thiringer, and M. Bongiorno, "Battery loss and stress mitigation in the cascaded H-Bridge multilevel inverter for vehicle traction applications by filter capacitors," IEEE Trans. Transport. Electrific., vol. 5, no. 3, pp. 659–671, Sep. 2019.

[9]. F. P. Feletto, R. A. Durham, E. d. C. Bortoni, and J. G. de Carvalho Costa, "Improvement to MV cascaded H-Bridge inverter (CHBI) VFD availability for high-power ESP oil wells," IEEE Trans. Ind. Appl., vol. 55, no. 1, pp. 1006–1011, Jan./Feb. 2019.

[10]. M. Sharifzadeh, G. Chouinard, and K. Al-Haddad, "Compatible selective harmonic elimination for three-phase four-wire NPC inverter with DC-Link capacitor voltage balancing," IEEE Trans. Ind. Informat., to be published. doi: 10.1109/TII.2019.2934467.

[11]. R. K. Beniwal, M. K. Saini, A. Nayyar, B. Qureshi, and A. Aggarwal, ''A critical analysis of methodologies for detection and classification of power quality events in smart grid,'' IEEE Access, vol. 9, pp. 83507–83534, 2021.

[12]. J. Y. Yong, V. K. Ramachandaramurthy, K. M. Tan, and N. Mithulananthan, ''A review on a state-of-the-art technologies of electric vehicle, its impacts and prospects,'' Renew. Sustain. Energy Rev., vol. 49, pp. 365–385, Sep. 2015.

[13]. Y. Qi, G. Mai, R. Zhu, and M. Zhang, ''EVKG: An interlinked and interoperable electric vehicle knowledge graph for smart transportation system,'' Trans. GIS, vol. 27, no. 4, pp. 949–974, Jun. 2023.

[14]. M. H. Nikkhah and M. Samadi, ''Evaluating an effect of electric vehicle charging station locations on line flows: An analytical approach,'' in Proc. 30th Int. Conf. Electr. Eng. (ICEE), May 2022, pp. 287–291.

[15]. S. Habib, M. Kamran, and U. Rashid, ''Impact analysis of vehicle-togrid technology and charging strategies of electric vehicles on distribution networks—A review,'' J. Power Sources, vol. 277, pp. 205–214, Mar. 2015.

[16]. F. Garcia-Torres, D. G. Vilaplana, C. Bordons, P. Roncero-Sánchez, and M. A. Ridao, ''Optimal management of microgrids with external agents including battery/fuel cell electric vehicles,'' IEEE Trans. Smart Grid, vol. 10, no. 4, pp. 4299–4308, Jul. 2019.

ISSN: 2582 - 4201(Online) , http://www.ijrdes.com/ , IJRDES, Vol. 7, ICETM 2025 , https://doi.org/10.63328/IJRDES-V7CIP16

[17].S.-A. Amamra and J. Marco, ''Vehicle-to-grid aggregator to support power grid and reduce electric vehicle charging cost,'' IEEE Access, vol. 7, pp. 178528–178538, 2019.

[18].C. Liu, K. T. Chau, D. Wu, and S. Gao, ''Opportunities and challenges of vehicle-to-home, vehicle-to-vehicle,and vehicle-to-grid technologies,'' Proc. IEEE, vol. 101, no. 11, pp. 2409–2427, Nov. 2013.

[19].S. Shahriar, A. R. Al-Ali, A. H. Osman, S. Dhou, and M. Nijim, ''Machine learning approaches for EV charging behavior: the review,'' IEEE Access, vol. 8, pp. 168980–168993, 2020.

[20].K. Ginigeme and Z. Wang, ''Distributed optimal vehicle-to-grid approaches with consideration of battery degradation cost under real-time pricing,'' IEEE Access, vol. 8, pp. 5225–5235, 2020.

[21].P. Sinha, K. Paul, S. Deb, and S. Sachan, ''Comprehensive review based on an impact of integrating electric vehicle and renewable energy sources to a grid,'' Energies, vol. 16, no. 6, p. 2924, Mar. 2023.

[22].J. James, J. Lin, A. Y. Lam, and V. O. Li, ''Maximizing aggregator profit through energy trading by coordinated electric vehicle charging,'' in Proc. IEEE Int. Conf. Smart Grid Commun. (SmartGridComm), Sydney, NSW, Australia, May 2016, pp. 497–502.

[23].Y. Vardanyan, F. Banis, S. A. Pourmousavi, and H. Madsen, ''Optimal coordinated bidding of the profit-maximizing EV aggregator under uncertainty,'' in Proc. IEEE Int. Energy Conf. (ENERGYCON), Limassol, Cyprus, Jun. 2018, pp. 1–6.

[24].T. Mao, X. Zhang, and B. Zhou, ''Intelligent energy management algorithms for EV-charging scheduling with consideration of multiple EV charging modes,'' Energies, vol. 12, no. 2, p. 265, Jan. 2019.

[25].Z. Moghaddam, I. Ahmad, D. Habibi, and Q. V. Phung, ''Smart charging strategy for electric vehicle charging stations,'' IEEE Trans. Transport. Electrific, vol. 4, no. 1, pp. 76–88, Mar. 2018

[26].N. Peddinti and S. Ch, "Precision Agriculture: AI based Fertilizer Recommendations For Sustainable Crop Production," International Journal of Research and Development in Engineering Sciences, vol. 7, no. 3, p. 40, Jun. 2025, doi: 10.63328/ijrdes-v7ri3p8.

[27].S. K. Palla and P. L. Mareddy, "Solar-Powered Electric Vehicle-Integrated sprayer system for sustainable Small-Scale and horticultural farming," International Journal of Research and Development in Engineering Sciences, vol. 7, no. 2, p. 47, Mar. 2025, doi: 10.63328/ijrdes-v7ri2p9.